Collectivity in light zirconium isotopes: Evolution with neutron number and angular momentum

A. A. Chishti, P. Chowdhury, D. J. Blumenthal, P. J. Ennis,* C. J. Lister, and Ch. Winter*
A. W. Wright Nuclear Structure Laboratory, Yale University, 272 Whitney Avenue, New Haven, Connecticut 06511

D. Vretenar†
Physics Department, Technical University of Munich, D-85748 Garching, Germany

G. Bonsignori and M. Savoia
Istituto Nazionale di Fisica Nucleare, Sezione di Bologna and Department of Physics, University of Bologna, Bologna, Italy
(Received 11 June 1993)

Considerable data have recently been collected on light zirconium isotopes. We present new measurements on ^{84}Zr and some unpublished results on ^{82}Zr. We have performed calculations on ^{82,84,86}Zr using an extension to the IBM which allows a collective core to couple to up to four unpaired fermions (two broken pairs). The role of vibrational collectivity is clear in the $N=44$ and $N=46$ nuclei, but collective rotation becomes the dominant mode below $N=44$. The relative positions of the neutron and proton Fermi surfaces are crucial in determining the complexity of the decay path down the yrast states, being dominated by proton configurations for $N\leq 44$ but showing strong competition between neutron and proton structures when $N>44$.

PACS number(s): 21.10.Re, 23.20.−g, 21.60.Fw, 27.50.+e

I. INTRODUCTION

The zirconium isotopes from mass 80 to 102 provide an excellent opportunity to study the microscopic causes of collective motion in nuclei. They are sufficiently heavy that substantial collective motion occurs, yet are susceptible to modulation by shell structure so all types of nuclear excitation are found. Near $N=Z=40$, the ground-state shapes are very highly deformed, with a quadrupole deformation of $\beta_2\approx 0.4$ and the spectra are dominated by rotational collectivity. With increasing neutron number, rotational effects diminish rapidly and the nuclei are soft to vibrations. Near $N=50$, the nuclei become rigidly spherical and single-particle excitations are the dominant mode of excitation, with no evidence of collectivity, even at the highest spin. In heavier isotopes, sphericity persists between $N=50$ and $N=56$, with susceptibility to octupole collective vibrations, and finally, beyond $N=56$, a dramatic transition back to deformation occurs and the nuclei once more have very large ground-state deformation.

The experimental studies of this unusual chain of isotopes have been matched by detailed theoretical investigations. For the stable, spherical nuclei near $N=50$, shell-model calculations have been performed for some time (see Warburton *et al.* [1] and references therein), but a comprehensive understanding of the whole sweep of nuclei in a single theoretical framework has only recently been attempted. Considerable progress in this direction is being made through the development of large Hartree-Fock calculations with realistic forces [2,3], and analysis of low-spin states in the interacting boson model (IBM) formalism [4,5]. However, the approach which has been most successful to date has been the sophistication of macroscopic-microscopic cranking calculations [5–8]. They have proven very powerful, especially in predicting the shapes and binding energies of nuclei with deformed mean fields. However, these mean-field calculations have shortcomings, especially when the coupling of vibrational and single-particle degrees of freedom to the motion of the mean field become important. This is most apparent when several modes of excitation are in competition. A microscopic understanding of the interactions between the different modes of excitation, and how polarization of the mean field is driven, would be highly desirable. The competition between the various modes of excitation lead to levels having complex wave functions with amplitudes arising from each mode. These amplitudes can frequently be extracted from electromagnetic transition matrix elements which are the experimental observables through which the interactions are explored. In this paper we discuss an approach in which these couplings, and the resulting structures, can be investigated in considerable detail. The theoretical model is an extension of the IBM to high-spin physics which allows the interaction of collective bosons and up to four decoupled fermions to be studied. As compared to traditional models based on the cranking scheme, this approach has the advantage that all calculations are performed in the laboratory system and provide results directly comparable with experimental quantities. The model has been applied to well-deformed systems [9], but is especially relevant for transitional regions where single-particle and vibrational col-

*Present address: AT&T Bell Labs, 101 Crawfords Corner Road, Holmdel, NJ 07733.
†On leave of absence from Physics Department, University of Zagreb, Croatia.

lectivity are the dominant modes of excitation and no clear axis for cranking exists. Our approach has been tested in the analysis of transitional mercury nuclei [10-12], and in this work we expand on our analysis [13] of transitional zirconium nuclei.

This paper discusses a detailed investigation of the lighter zirconium nuclei between $N=42$ and 48 where a change from rotational through vibrational to single-particle dominated spectra is found. The work is divided into two parts: in the first part is a presentation of unpublished experimental measurements on ^{82,84}Zr and a review of the experimental situation. Some erroneous assignments in the literature are corrected and relevant new information is added. Then, working from our detailed analysis of ^{86}Zr which has been published previously [13], we discuss calculations of the lighter isotopes and our insights of the evolution of structure.

II. NEW INFORMATION ON ^{84}Zr

A. Study of high-spin states

The level scheme of ^{84}Zr was investigated through the ^{58}Ni (^{29}Si,$2pn$)^{84}Zr reaction by bombarding ^{58}Ni targets with ^{29}Si ions at $E_{\text{beam}}=110$ MeV from the Tandem Accelerator Superconducting Cyclotron (TASCC) facility at Chalk River. The target consisted of two stacked foils of enriched ^{58}Ni, each foil being 230 μg/cm^2 thick. Gamma rays were detected in the 8π spectrometer which consists of 20 Compton-suppressed HP germanium detectors positioned at angles of 37°, 79°, 101°, and 143° with respect to the beam axis and an inner ball of 70 BGO detectors acting as a multiplicity filter and gamma-ray calorimeter. A 16-element CsI charged particle detector array (ALF) was mounted inside the BGO ball. These detectors were positioned in three rings at 45°, 90°, and 135°. More details on the spectrometer can be found in Refs. [14,15].

An event was recorded only if it consisted of coincident signals from at least two Ge detectors, at least five elements of the BGO calorimeter, and a signal from at least one particle detector. A total of 62.4 million events satisfying these requirements was recorded for further analysis. In the off-line analysis, an E_γ vs E_γ matrix of Ge-Ge coincidences was created with a more stringent requirement of at least 13 BGO elements firing, as well as an identified proton in one of the charged-particle detectors. Evaporated protons were discriminated from α particles by pulse-shape analysis. Under these conditions, we were able to significantly suppress the $\alpha 2p$ and $\alpha 2pn$ evaporation channels leading to ^{80,81}Sr.

Matrices were created to provide information on the multipolarity of the emitted radiation. The symmetry of the array provided two angles, 37° (and 143°) and 79° (and 101°) for this analysis. All transitions were examined by measuring their intensity observed at each of these angles in coincidence with other members of the groundstate band sequence. Table I shows the result of this analysis.

TABLE I. Energies and angular momentum properties of transitions and states in ^{84}Zr. The DCO ratios are described in Sec. II A and angular distribution measurements in Sec. II B.

E_x (keV)	E_γ (keV)	J_i^π	J_f^π	I_γ	Br	DCO	a_2	A_4
			Ground-state band					
540	539.7(1)	2^+	0^+	1000	100	0.82(2)	0.27(1)	−0.10(2)
1 263	722.9(1)	4^+	2^+	880(90)	100	0.83(2)	0.36(2)	−0.18(2)
2 136	873.7(1)	6^+	4^+	630(65)	100	0.83(2)	0.32(3)	−0.16(3)
3 089	952.7(1)	8^+	6^+	430(44)	100	0.89(2)	0.37(3)	−0.10(4)
4 069	979.8(1)	10^+	8^+	410(42)	100	0.87(3)	0.37(3)	−0.10(4)
5 136	1 067.2(1)	12^+	10^+	350(37)	100	1.03(5)		
6 303	1 166.5(1)	14^+	12^+	260(27)	100	0.88(2)		
7 498	1 195.6(1)	16^+	14^+	180(20)	100	0.86(2)		
8 744	1 245.7(2)	18^+	16^+	96(9)	100	0.81(2)		
10176	1 431.7(3)	20^+	18^+	88(8)	100	0.91(3)		
11821	1 645.9(3)	22^+	20^+	44(5)	100	0.88(4)		
13667	1 845.3(6)	24^+	22^+	17(8)	100	0.87(6)		
15660	1 993.5(6)	26^+	24^+	9(3)	100	0.76(8)		
			Odd-spin sideband					
3494	668.2(3)	(7^-)	(5^-)	44(5)	21(3)	0.68(5)		
4379	884.8(1)	(9^-)	(7^-)	140(14)	100	0.60(2)		
5317	937.7(1)	(11^-)	(9^-)	190(20)	>90	0.68(2)		
6325	1008.2(3)	(13^-)	(11^-)	90(7)	100	0.70(5)		
7412	1086.6(2)	(15^-)	(13^-)	110(10)	100	0.79(4)		
			Even-spin sideband					
3314	487.4(2)	(6^-)	(5^-)	80(8)	100	2.04(5)		
4036	722.3(5)	(8^-)	(6^-)	100(15)	72(7)	0.80(5)		
4867	832.3(5)	(10^-)	(8^-)	170(17)	71(3)	0.63(2)		
5783	915.5(2)	(12^-)	(10^-)	160(16)	90(4)	0.72(2)		
6794	1011.5(2)	(14^-)	(12^-)	140(14)	80(2)	0.69(2)		

The majority of the transitions are consistent with stretched quadrupole decays. The DCO ratios of the gsb are consistent with a sequence extending to spin $J^{\pi}=26^{+}$. To ascertain the spins and parities of the sidebands a polarization measurement of the interband transitions would be highly desirable and is planned. The measured g factor [21] of the $J^{\pi}=(5^{-})$ state of $1.4\pm0.4\mu$ supports the suggestion of a proton (fp-g) excitation with a negative-parity assignment. The sidebands themselves consist of stretched quadrupole decays but the level assignments are shown in parentheses in Fig. 1 due to the uncertainty of the bandhead spin and parity.

Two other experiments were performed at Daresbury Laboratory, U.K., which produced ^{84}Zr strongly. In the first experiment, a search for very high-spin states was performed by a Manchester/Daresbury collaboration with the TESSA array, repeating the study of Price *et al.* [16], but with considerably enhanced γ-ray efficiency. The states reported above spin $J^{\pi}=26^{+}$ were not confirmed [17]. A further experiment using the POLYTESSA array at the Recoil Separator produced an enormous amount of data on ^{84}Zr at low spin. A positive-parity sideband feeding into the ground-state band at spin 12^{+} was observed, as is also found in this work, but states at very high spin were not strongly populated [18].

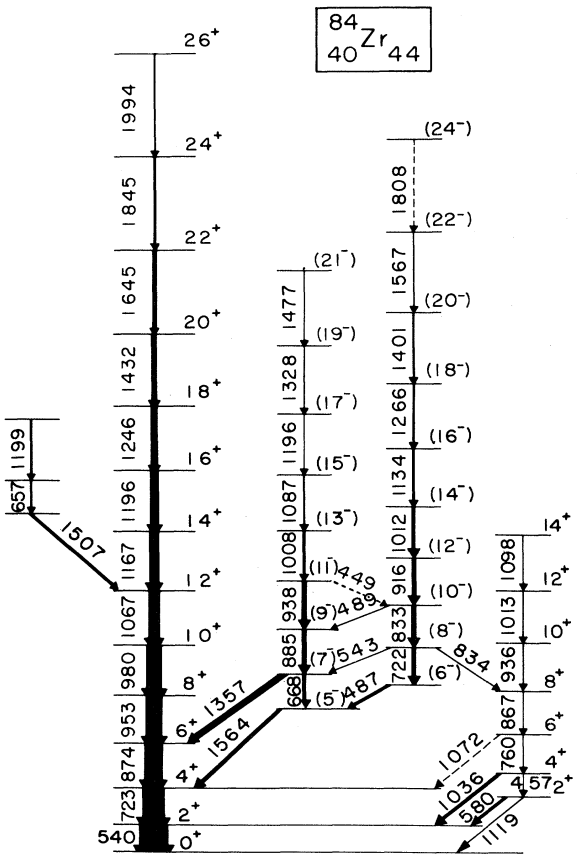

FIG. 1. The decay scheme for ^{84}Zr constructed from the recent experiments described in Sec. II.

B. Angular distribution measurements

In a separate experiment, using the ^{58}Ni+^{32}S reaction, low-lying states in ^{84}Zr were also populated through the $\alpha 2p$ evaporation channel. This experiment was performed at Yale University using the ESTU tandem accelerator to bombard 40-mg/cm^2-thick ^{58}Ni targets with ^{32}S ions at a beam energy of 110 MeV. The emitted gamma rays were detected at eight different angles between 100° and 149°, with four Compton-suppressed germanium detectors mounted on a rotatable frame. This arrangement allowed measurements at four different angles simultaneously. The details of this experiment can be found in Ref. [19]. The results of angular distributions for ^{84}Zr extracted from this experiment were found to be consistent with the previously reported [16] spin assignments. The angular distribution coefficients of the low-lying gsb transitions are given in Table I and are consistent with a stretched quadrupole cascade. The majority of the sideband transitions were too weak to be reliably extracted.

C. g-factor measurements

Using the transient field technique, Mountford *et al.* [20,21] have measured the yrast state g factors in ^{84}Zr up to spin $14\hbar$, high enough to unambiguously identify the first band crossing to be due to the alignment of a pair of $g_{9/2}$ protons. These low-lying nuclear states of interest were populated in the ^{54}Fe(^{33}S,$2pn$)^{84}Zr reaction at $E_{\text{beam}}=105$ MeV provided by the tandem accelerator at Daresbury Laboratory. An 8-μm-thick pure ^{54}Fe foil polarized by an electromagnet of 0.16 T, was used as a target. The details of this experiment have already been published [20] and we will discuss only the implications of these results in this paper.

D. Decay scheme for ^{84}Zr

The decay scheme constructed from the numerous sources mentioned in Sec. II is shown in Fig. 1. In overall structure it is similar to that reported in the pioneering work of Price *et al.* [16], but several discrepancies have become clear. Although the data from the Chalk River experiment were statistically superior by more than an order of magnitude, the states reported [16] above spin 26^{+} could not be verified, nor have they been verified in the other experiments discussed in Sec. II. Figure 2 clearly illustrates the lack of population of states above the level with spin $J^{\pi}=26^{+}$ which decays by a 1994-keV γ ray. In the $16^{+}\rightarrow 26^{+}$ spin regime, the previously reported transitions were apparently not sufficiently corrected for Doppler shifts, and a considerable discrepancy in transition energies was found. A new cascade was found to feed into the ground-state sequence at spin 12^{+} [see Fig. 3(b)], with 2% of the $2^{+}\rightarrow 0^{+}$ transition intensity. This cascade had not been reported in the earlier work, although the intensity is stronger than that of the states claimed to have been seen above spin 24^{+}, the $26^{+}\rightarrow 24^{+}$ decay being 1% of the $2^{+}\rightarrow 0^{+}$ decay. At a similar intensity level, the negative-parity sidebands also showed discrepancies from

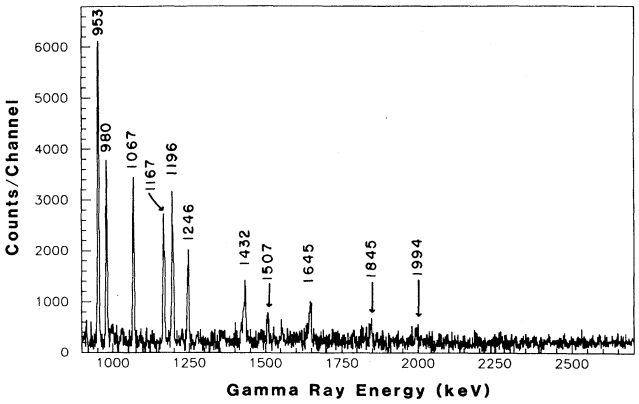

FIG. 2. Sum of clean gates (980-, 1067-, 1167-keV transitions) from the ground-state band illustrating the rapid decrease in population of the yrast sequence above spin $26\hbar$.

those reported. Figure 3(a) shows an example of our data, in which the absence of the previously reported [16] 1260-keV γ ray is apparent. Our statistically superior data allowed us to extend all sidebands to higher spin, although, as mentioned earlier, no states above spin 26^+ were found in the ground-state sequence.

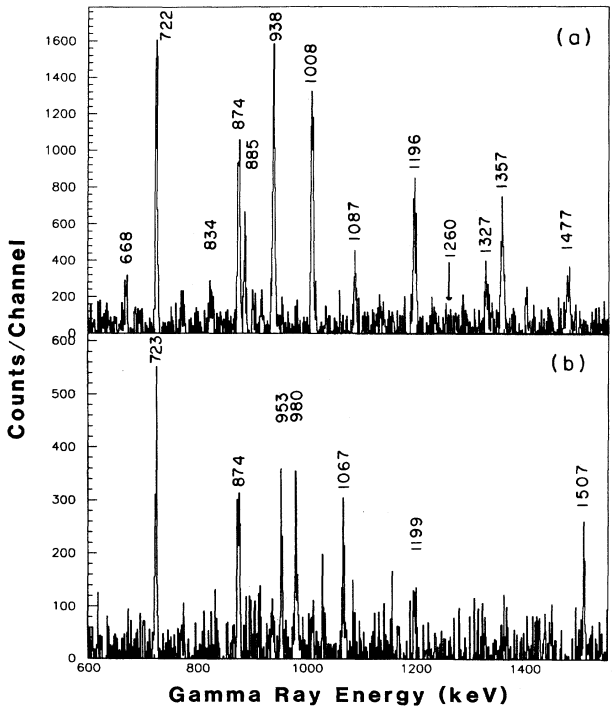

FIG. 3. Examples of coincident gamma-ray spectra used for reconstructing the decay sequence for ^{84}Zr. (a) Sum of gates of 885- and 1087-keV transitions in the negative-parity states which illustrate the rotational-like pattern of decays. The absence of 1260-keV transition is clear from this spectrum. (b) Energy spectrum created by gating on the 657-keV transition of the proposed cascade feeding into the ground-state band.

III. NEW INFORMATION ON ^{82}Zr

Excited states in ^{82}Zr were first reported by Lister *et al.* [22]. They used the ^{58}Ni(^{28}Si,$2p2n$) reaction at 120 and 125 MeV to populate these states. Candidates for the first three excited states were found in $2n$-, $2p$-, and $2pn$-gated spectra. The cross section for populating the first excited state was estimated to be 8 ± 2 mb at 125 MeV. A further experiment was performed to measure the lifetimes of these states using the recoil distance method which has not been previously published. The lifetime of the first excited state was measured as $\tau_m=40\pm4$ ps and the second as $\tau_m=8\pm2$ ps. These measurements have become relevant in the context of this work and with the publication of a more detailed investigation of the decay scheme by Mitarai *et al.* [23]. Using the same reaction, but a much more efficient spectrometer, they were able to trace the evolution of the ground-state band to spin $J=20\hbar$. Both the rotational-like sequence of states and the $B(E2{:}2^+\rightarrow0^+)=1840\ e^2\text{fm}^4$ indicate that the ground state has a deformed shape.

IV. INTERPRETATION OF THE RESULTS

A. CSM calculations

A very thorough analysis of ^{84}Zr was performed by Dudek *et al.* [8] in the cranked shell-model (CSM) formalism. Most of the key conclusions of their work remain unaltered by the revisions to the decay scheme found in the more recent experiments reported herein. In particular, the conclusion that the nucleus has a very poorly defined, soft mean-field shape at low spin is corroborated. Further, the conclusion that the first alignment in the yrast sequence and the negative-parity states are proton excitations are borne out by the g-factor measurements [20] and are consistent with the IBA approach we discuss in Section IV B 2. However, the absence of identified states above spin 26^+ in the yrast sequence and the improved data on negative-parity bands make some of the discussion of particle alignments at higher spin and pairing reduction more speculative. The revised $J^{(1)}$ and $J^{(2)}$ moments of inertia are plotted in Fig. 4 using the results of the present study. These plots clearly indicate the absence of a second upbend in the unfavored cascade of negative-parity states reported in the old data. Certainly several key questions concerning the location of superdeformed states and the reduction of pairing remain to be answered.

B. The interacting boson model plus broken pairs interpretation

The model we have used to analyze the states in ^{82,84,86}Zr is described in detail in Refs. [9,11]. In short, it is based on the IBM-1 in which fermions couple pairwise to form s and d bosons, with no distinction between protons and neutrons [24,25]. To compute high-spin states, the model allows one or two bosons to be destroyed and form noncollective fermion pairs, represented by two- and four-quasiparticle states which can recouple to their

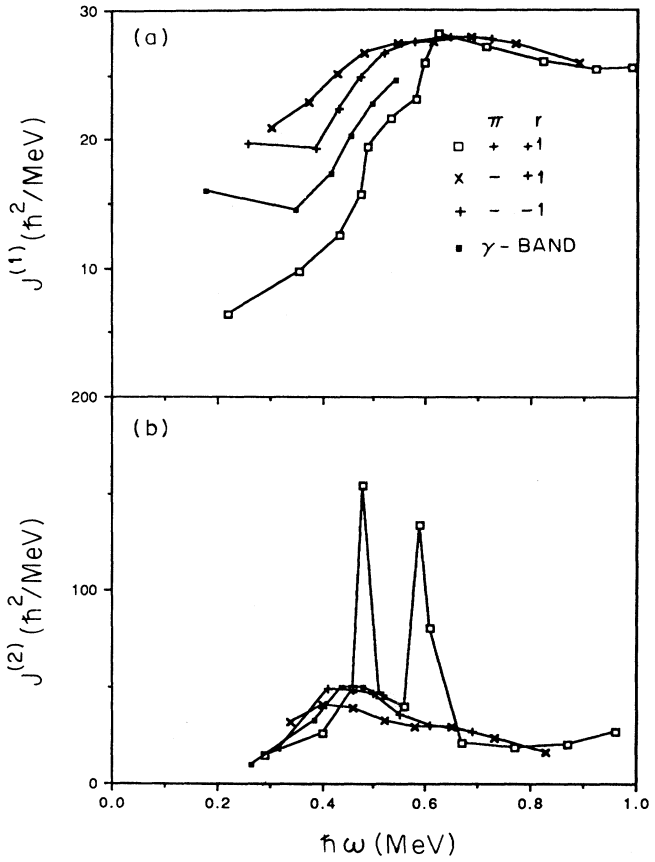

FIG. 4. The two moments of inertia ($J^{(1)}$ and $J^{(2)}$) for the four cascades in ^{84}Zr derived from the present decay scheme. At rotational frequencies above $\hbar\omega \cong 0.56$ MeV they differ considerably from that discussed in Refs. [8,16].

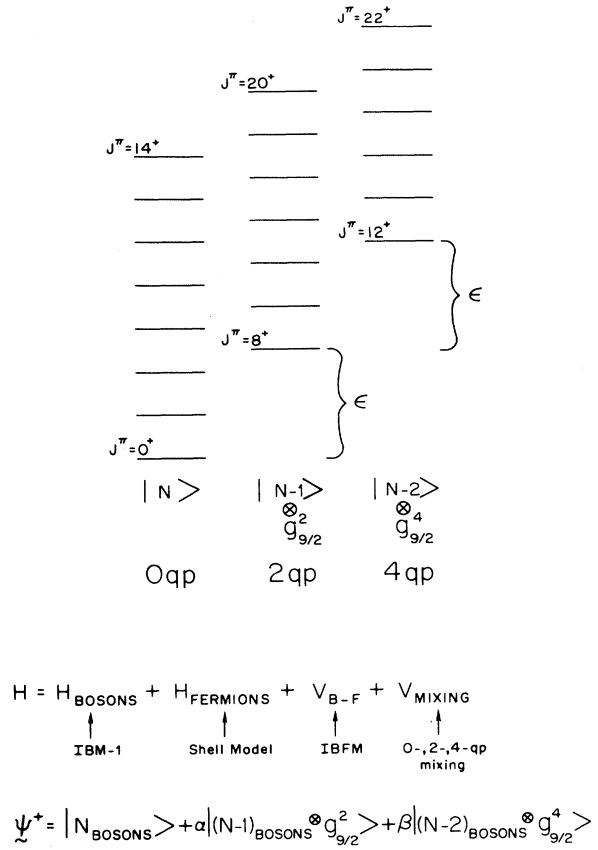

FIG. 5. Schematic picture of our theoretical model and Hamiltonian.

respective boson cores. In the present model, we can only separately consider neutron or proton excitation and not mixed configurations. Figure 5 schematically shows the structure of the Hamiltonian and the expected sets of levels. The Hamiltonian has four terms: a bosonic part, a fermionic part, a boson-fermion interaction and a pair-breaking interaction which mixes 0qp, 2qp, and 4qp configurations. The form and strength of most of the interactions is well established. As far as has been possible, the collective core parameters and boson-fermion couplings have been taken from previous analyses of low-spin states in neighboring even and odd A nuclei [4,5]. In Table II, we display the model Hamiltonian parameters used in the present calculation for the zirconium isotopes. The parameters of the IBM-1 boson core Hamiltonian are very close to the values that were used in Ref. [4] for the description of low-spin states in strontium isotopes. The isotonic Sr and Zr nuclei have the same number of bosons in the IBM representation and their energy spectra are very similar. For ^{82}Zr there are not enough experimental data to fix the core parameters. For this nucleus we have used the ^{80}Sr parameters [4]. The single-quasiparticle energies and occupation probabilities are determined from a simple BCS calculation using Kisslinger-Sorensen [26] single-particle energies and pair-

TABLE II. The parameters used in the extended IBFM calculations described in this work. All values are in MeV except the boson number and occupation probabilities.

Parameter	^{86}Zr	^{84}Zr	^{82}Zr
N	7	8	9
ε	0.74	0.59	0.41
c_0	0.6	0.2	0.2
c_2	−0.23	−0.23	−0.1
c_4	0.12	0.14	0.13
v_0	−0.2	−0.1	−0.2
v_2	0.14	0.07	0.11
$\varepsilon(g_{9/2})P$		1.6	1.6
v_2		0.22	0.22
$\varepsilon(g_{9/2})N$	1.6		
v_2	0.63		
$\varepsilon(p_{1/2})P$		1.33	1.33
v_2		0.53	0.53
$\varepsilon(p_{1/2})N$	1.2		
v_2	0.92		
Γ_0	0.3	0.3	0.3
χ	−1.0(N)	0.9(P)	0.9(P)
λ	0.5	4.0	4.0
A_0	0.015	0.005	
u_0	1.5	0.7	0.7
u_2	0.1	0.25	0.25
v_0	−0.5	−0.5	−0.5

ing strength $G=24/A$. As one would expect from the experimental spectra, the fermion orbitals particularly relevant in the description of 2qp and 4qp states close to the yrast line are the $g_{9/2}$ and $p_{1/2}$. These two orbitals lie closest to the Fermi level. In order to reduce the large size of the 4qp space, only the $g_{9/2}$ orbital is included in the calculation of positive-parity states. The $p_{1/2}$ and $g_{9/2}$ orbits form the fermion space in the calculation of negative-parity bands. To reproduce the excitation energies of the 8^+ states [bandheads of the $(g_{9/2})^2$ configurations], we had to renormalize the neutron single-quasiparticle energies. The proton states were correctly reproduced and needed no modification. The strength parameter of the boson-fermion dynamical interaction Γ_0 and the parameter of the boson quadrupole operator χ are similar to those used by Bucurescu *et al.* [4] for the description of low-spin states in odd Y and Sr isotopes. The positions of the low-lying $J^\pi=\frac{5}{2}^+, \frac{7}{2}^+, \frac{9}{2}^+$ states in these nuclei determine the rather large value for the strength parameter Λ_0 of the boson-fermion exchange interaction. In ^{86}Zr we found that it was necessary to reduce Λ_0 to a very small value. We will discuss this reduction in Sec. IV B 1. For the negative-parity states in ^{86}Zr and ^{84}Zr a weak monopole boson-fermion interaction was included that increases the moment of inertia of the lowest bands. The residual interaction between fermions is the surface δ interaction with the strength parameter $v_0=-0.5$ MeV. This parameter is determined primarily from the energy spacings of states of opposite signatures in the negative-parity bands. The pair-breaking interaction that mixes states with 0qp, 2qp (one broken pair), and 4qp (two broken pairs), is relatively weak and the mixing between configurations with different number of unpaired fermions is small.

The low-spin states in strontium and zirconium isotopes have been analyzed in the context of the IBM-1 (Ref. [4]) and using IBM-2 (Ref. [5]). For both strontium and zirconium isotopes, the number of neutron bosons, counting from the $N=50$ shell, varies from five to two as one moves from midshell toward the $N=50$ shell closure, while the proton boson number remains constant at five. In this transitional region the collective core changes considerably, being nearer the rotational SU(3) limit for $N=40,42$ and nearer the vibrational U(5) limit for $N=44,46$. Neither extreme is reached in nuclei in this region, however, and large anharmonicities corresponding to geometrical triaxial softness are always present. It should be noted that a better understanding of the collectivity of these nuclei at modest excitation energies needs more data on the states of low spin, which are very sensitive to structure.

1. *Discussion of ^{86}Zr*

In their detailed study of ^{86}Zr, Chowdhury *et al.* [13] have shown that the states up to the highest observed spins (about $24\hbar$) arise from anharmonic collective vibrations coupling to aligned quasiparticles. The spectra do not show any clear signs of an evolution of core collectivity with spin.

The very large $B(M1)$ transitions in the four-quasiparticle regime are particularly unusual and can only be caused by several aligned particles in the $g_{9/2}$ orbit. The rather weak coupling between 0qp, 2qp, and 4qp states results in a prediction of suppressed $B(E2)$ matrix elements between configurations. Although the data show less abrupt discontinuities, the trend in matrix elements is fairly well reproduced. Figure 6 shows a comparison of experiment and our calculation. Geometrical models of any fixed shape do not reproduce the measurements and would require an evolution of shape from state to state. In addition to the transitional electric and magnetic moments, we have calculated the static magnetic moments of states. These are interesting, as unlike the transitional $B(M1)$ matrix elements, which are found to be similar for quasineutron and quasiproton configurations due to a cancellation of spin and orbital terms, the static moments allow unambiguous assignments of the nature of the aligned quasiparticles. Measurements of the static magnetic moments of low-lying states are in progress, using both static and transient fields [27,29]. These measurements show our assignments of aligned $g_{9/2}$ proton and neutron states to be correct. Table III gives the calculated static magnetic moments for ^{82,84,86}Zr.

The coupling of bosons and fermions in this mass region has been examined [28] through analyzing the low-spin states in odd-A nuclei with the IBFM. In order to reproduce the four-quasiparticle spectrum of ^{86}Zr, we found a reduction of the exchange term of the coupling interaction was necessary, from $\Lambda_0=3.7$ to 0.5 MeV. This was not discussed in detail in our work [13]. In order to understand its origin, one may consider the coupling of unpaired neutrons to neutron bosons in the ^{86}Zr core. In the ground state, there are two neutron bosons to which odd neutrons would couple through the exchange interaction, for example, in ^{85}Zr. However, to create multineutron states in the even-even nucleus we destroy neutron bosons and the effective coupling of the exchange interaction is reduced. In the IBM-2 framework this reduction would be implicit and no adjustment

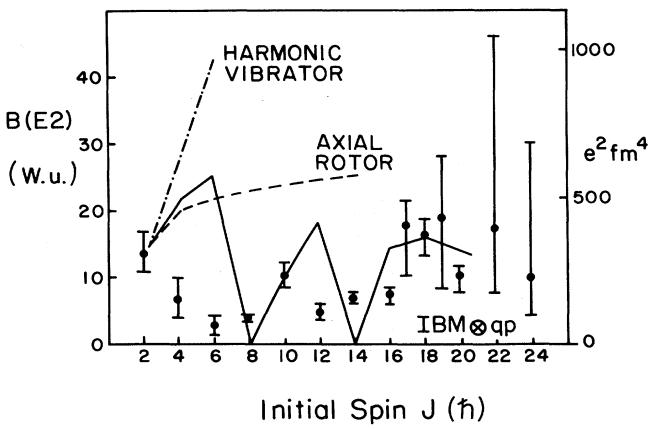

FIG. 6. $B(E2)$ strengths measured for the yrast sequence in ^{86}Zr compare to geometrical models and to the present calculation.

TABLE III. g factors calculated for low-lying states in ^{86,84,82}Zr. The ^{84}Zr measurements are taken from Ref. [21].

Spin (J)	^{86}Zr Calc.	^{84}Zr Calc	^{84}Zr Expt.	^{82}Zr Calc.
2^+	0.46	0.48	0.5±0.1	0.49
4^+	0.46	0.48	0.4±0.3	0.49
6^+	0.46	0.48	1.9±0.11	0.49
8^+	−0.22	0.48	1.5±0.6	0.49
10^+	−0.09	0.88	0.5±0.8	0.49
12^+	0.00	0.87	0.9±0.7	0.51
14^+	−0.19	0.85	1.3±0.5	0.78
$8^+,10^+,12^+,14^+$ average		0.77	0.87±0.1	
5^-	−0.18	1.19	1.4±0.4	

of strength parameters should be needed. However, in our model based on IBM-1, we couple to all the core bosons, irrespective of their nature and the suppression of coupling is greatly diminished; thus, the need to empirically reduce the strength of coupling parameter to account for this effect. In the case of four-quasineutron states in ^{86}Zr, this effect is particularly pronounced, as all the neutron core bosons are destroyed, and coupling to like fermions should vanish. When the number of core bosons of the same type as the unpaired fermions is large, the reduction of the effective exchange interaction is less pronounced. This is the case for coupling proton states to the core in the lighter zirconium isotopes. Apart from this, we have followed the approach of working from our ^{86}Zr calculation [13] with as little modification of the model parameters as is possible, with the aim of ascertaining the change in structure with neutron number and angular momentum.

2. *Discussion of ^{84}Zr*

As we have seen in Sec. III, there is a considerable amount of new information on ^{84}Zr. At first appearance the ground state band in ^{84}Zr is very different from that of ^{86}Zr. A single cascade of decays carries almost all the intensity and sidebands are relatively weak. The moment of inertia rises rather gently and has less pronounced irregularities. In contrast, ^{86}Zr has several decay paths and shows two very drastic changes in moment of inertia. One may initially think that the vibrational-like behavior of ^{86}Zr has changed to rotational collectivity in ^{84}Zr. This is indicated in the cranked shell-model calculations which reveal that the mean deformation at low spin has moved from $\beta_2=0$ in ^{86}Zr to $\beta_2=0.2$ in ^{84}Zr. However, the potential-energy surfaces are still very soft and only show well-developed minima [8] above spin $J=20\hbar$. Experimentally it is certainly the case and the low-lying states are soft to shape fluctuations. Thus, our IBM approach with anharmonic vibration may be the appropriate approach. Results from our calculations are shown in Fig. 7 in which the first ten states of each spin are shown. It reflects the shell-model origins of our calculation, and contrasts strongly with the sparse information on nonyrast states one is able to obtain from mean-field calculations. The collective gsb (0qp) remains yrast up to spin $J=8^+$. The 2qp band based on the proton configuration $[(\pi g_{9/2})2]_8$ becomes yrast at angular momentum $J^\pi=10^+$. This band remains yrast up to the highest calculated angular momenta. The four-quasiparticle states below spin $J=20\hbar$ are always 1–2 MeV above the yrast line. A detailed comparison of calculations with observed states in the positive- and negative-parity states is shown in Fig. 8.

The drastic change of the decay pattern and the differing moments of inertia in ^{86}Zr and ^{84}Zr, which are shown for the ground-state sequence in Fig. 9, can be easily interpreted in our model. They arise from a change in structure caused by the lowering of the Fermi level for neutrons between $N=46$ and 44. In the case of ^{86}Zr, the proton and neutron Fermi levels are such that

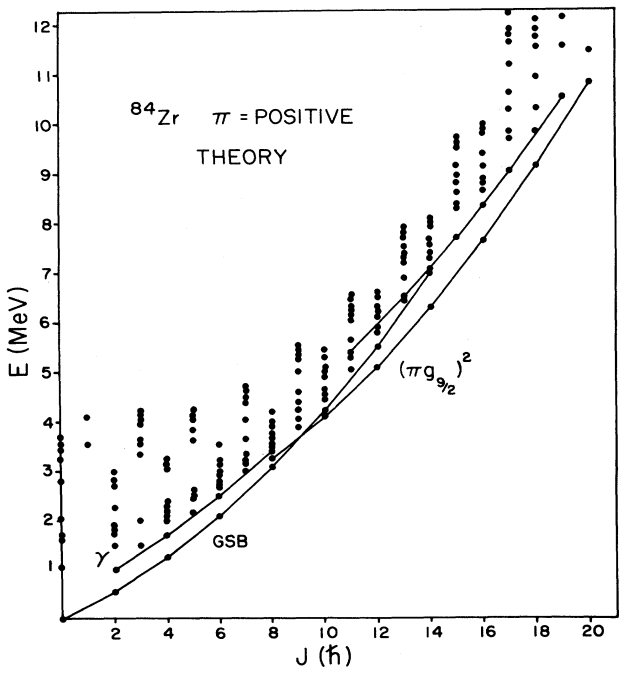

FIG. 7. Some of the positive-parity states calculated for ^{84}Zr. The first ten states of each spin, for configurations involving core vibrations coupled to quasiproton states, are shown.

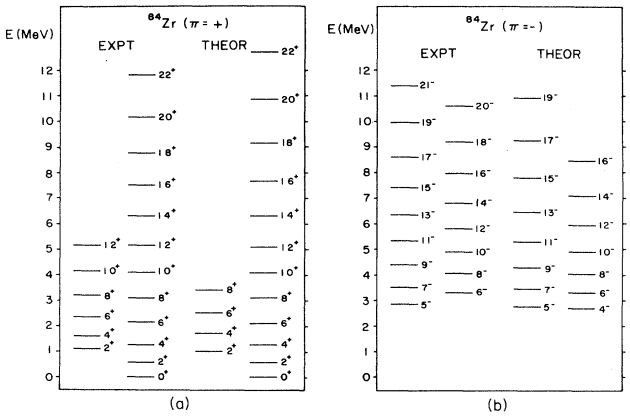

FIG. 8. A detailed comparison of states calculated for ^{84}Zr (a) in the positive-parity sequence (b) in the negative-parity sequence.

both types of quasiparticle excitations are very close, and the yrast sequence contains first no aligned particles, then aligned neutrons (above spin $8\hbar$ at 3299 keV) and protons (above spin $8\hbar$ at 3539 keV), then finally four-quasiparticle states (above spin $14\hbar$ at 6322 keV) which are probably a mixed proton and neutron configuration. In ^{84}Zr, which has two fewer neutrons, the neutron Fermi level is lower and more energy is needed to promote neutrons into the $g_{9/2}$ orbit. The two-quasineutron bandhead is calculated to lie at $\sim$3500 keV which is $\sim$400 keV above the yrast states. Consequently, aligned-proton states dominate the yrast sequence in the two-quasiparticle regime. Thus, comparing the yrast sequences is tantamount to comparing two different sets of levels. Figure 10 shows the comparison of the moment of inertia of 0qp and proton 2qp states in ^{84,86}Zr. Now a close similarity is found and there is also good agreement with predictions.

At the very highest spins in ^{84}Zr there appears to be a large increase in collectivity [16]. Our calculations indicate that these are not the states analogous to the four-quasiparticle yrast sequence observed in ^{86}Zr and other $N=46$ isotones. The main consequence of the strong exchange interaction is a decrease of the moment of inertia of bands based on aligned-fermion configurations as compared to the collective ground-state band. This is true for two-quasiparticle states, and an even stronger effect for four-quasiparticle states. Thus, although the lowest four-quasiparticle bandhead might be only slightly above the yrast levels, the 4qp band rises steeply and is apparently not populated. The sequence of states which have been seen are reported [16] to show a large increase in transitional quadrupole moment. If true, this probably reflects the large increase in core deformation to $\beta_2=0.35$ polarized by the aligned particles as predicted by the CSM calculations. Without core modification, such a large change in transition rates is difficult to reproduce in our model. The verification of this effect would be of considerable interest.

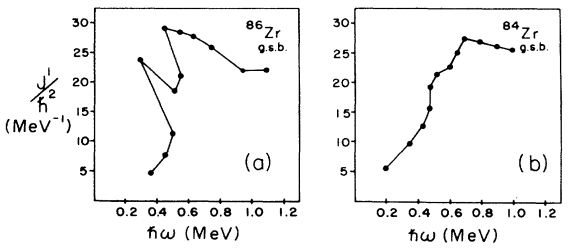

FIG. 9. The moments of inertia of the ground-state sequence in ^{86,84}Zr.

The quasi-gamma sequence of even-spin positive-parity states is well reproduced by our calculations. The odd-spin members of this band are of considerable significance in interpreting the gamma softness of the nucleus [30]. However, they are not populated and despite a careful search of the data, no convincing candidate could be found.

The negative-parity states are not as reported in Ref. [16]. Figure 1 shows the correct level sequence, with both bands extended to higher spin. Some of the irregular features interpreted [8] to be associated with neutron alignment have now been removed, and the moments of inertia slowly rise with angular momentum. In the cranking picture, evidence for neutron alignment is found in the ground-state band at a rotational frequency of $\hbar\omega\cong 0.58$ MeV while a similar alignment is apparently absent in the negative-parity bands which are of aligned-proton origin. It can only be accounted for by invoking considerably different shapes to the bands at this excitation energy. The negative-parity sequence of states is rather well described in our calculation, shown in Fig. 8(b). We find the states at the lowest spin can be reproduced by coupling the two-proton configuration $g_{9/2}$-$p_{1/2}$ coupled to the boson core vibrations. The decoupled proton nature of these states is confirmed by the measured [21] g factor for the $J^\pi=5^-$ state of $g=1.4(4)$. The analogous set of neutron states is expected to be nonyrast by more than 500 keV. This pattern of negative-parity states is similar to that of ^{86}Zr, although in ^{86}Zr the lowest states are predicted to be quasineutron excitations and have negative g factors (Table II). The inclusion of the proton $p_{3/2}$ orbit leaves the lowest states almost unmodified, but the admixtures increase with angular momentum.

In the work of Mountford *et al.* [20], transition strengths in the yrast sequence were remeasured. With one exception, that of the $J^\pi=10^+\rightarrow 8^+$ decay, the agreement with previous results is remarkably good and the experimental uncertainties reduced. Adopting the most recent result, the $B(E2)$ values show correspondence with our model predictions, the reduced $10^+\rightarrow 8^+$ strength arising from the change of configuration at the zero- to two-quasiparticle changeover. This sequence of matrix elements is extremely difficult to reproduce in any traditional vibrational or rotational calculation, but emerges naturally from our model. At low spin, even our IBM calculation does not reproduce well the experimental sequence of transitions between collective states. It may well be that at the lowest energies, the subshell gaps

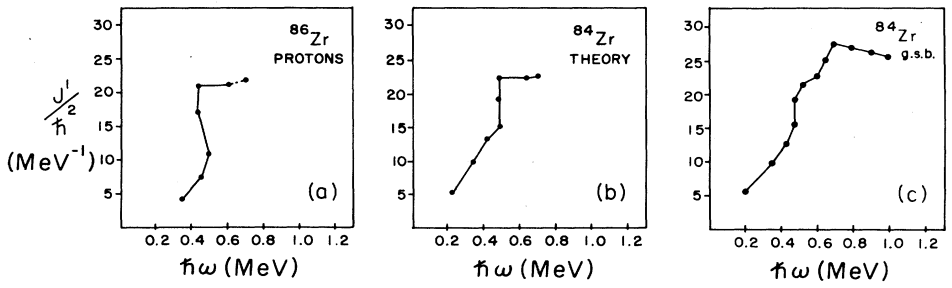

FIG. 10. A comparison of (a) experimentally known quasiproton states in ^{86}Zr, (b) calculated quasiproton states in ^{84}Zr, and (c) experimentally known quasiproton states in ^{84}Zr.

at nucleon number 38 and 40 play a role in reducing collectivity, and the core bosons should be recounted. Indeed, assuming a shell gap at nucleon number 38, only four core bosons allows an improved agreement to be obtained, as is also shown in Fig. 11, with strong boson saturation leading to a more rapidly decreasing set of matrix elements. This saturation effect is even stronger in the ^{86}Zr 2-4-6 sequence as can be seen in Fig. 6. Further, it appears that in the four-quasiparticle regime, no subshell effects are apparent. A more systematic analysis of this saturation problem is in progress and will be reported separately.

3. *Discussion of ^{82}Zr*

The information [22] on ^{82}Zr has recently been greatly extended [23]. Here, the deformation of the ground state has been established and the lifetimes of the first and second excited states reflect the fact, $B(E2{:}2^+\rightarrow 0^+)=1840\pm185$ $e^2\,\mathrm{fm}^4$, $B(E2{:}4^+\rightarrow 2^+)=993\pm253$ $e^2\,\mathrm{fm}^4$. The nucleus is still far from being a good rigid rotor and we have attempted a calculation of states to gain insight into their structure. Insufficient information on low-spin states is available to reliably describe the core collectivity, so we have resorted to information on ^{80}Sr, the $N=42$ isotone, and the analysis of it by Bucurescu *et al.* [4] for the boson hamiltonian parameters. All other parameters were taken from our analysis of ^{84}Zr and without any attempt to modify parameters to optimize the description of ^{82}Zr, we have obtained reasonable agreement with the data. Figure 12 shows our calculation and the data on ^{82}Zr and ^{80}Sr.

The most salient feature we find in examining the wave functions is a major change in the core states. The change towards the rotational SU(3) limit is manifested in the fragmentation of the core wave function into many boson amplitudes. This is a sharp difference from the situation nearer the vibrational limit where each angular momentum was dominated by just a few amplitudes. The effect of this fragmentation is a greatly increased overlap between core and aligned quasiparticle configurations, and considerably more mixing. Thus, the sharp drops in transition rates at the crossing points between configurations are significantly washed out. Again, proton alignment is predicted to dominate the states of intermediate spin in the two-quasiparticle regime, with the two-quasineutron states about 800-keV nonyrast. Finally, the aligned four-quasiparticle states of the type which dominated ^{86}Zr were again found to be nonyrast. The g factors (Table III) are predicted to be rather monotonic, following the collective value, then rising at spin $12\hbar$ and $14\hbar$ with proton alignment, and slowly declining again.

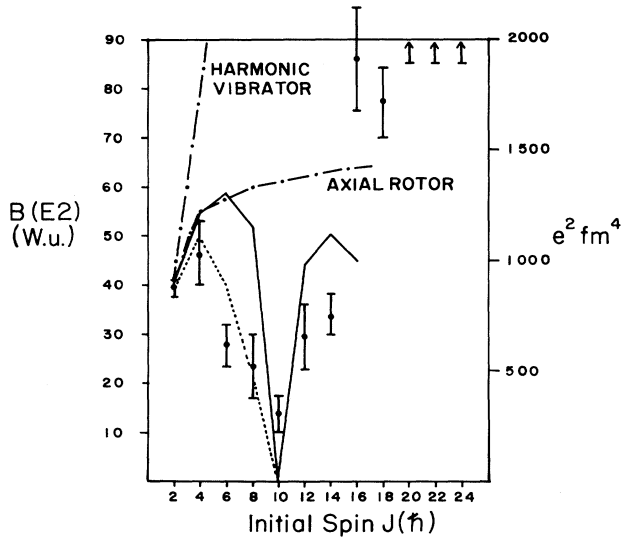

FIG. 11. A comparison of experimental $B(E2)$ values for ^{84}Zr along the ground-state sequence compared with geometrical models (—·—·—·), our calculation in the full 28–50 shell model space (——), and our calculation in a space truncated by the $Z=38$ subshell closure (· · · ·).

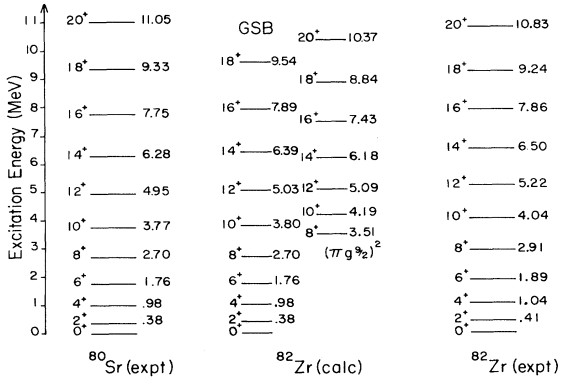

FIG. 12. The yrast sequence in the $N=42$ isotones. (a) ^{80}Sr experimental, (b) ^{82}Zr calculation, (c) ^{82}Zr experimental.

V. CONCLUSION

Considerable new data are available on light zirconium isotopes which allow new insight to be gained on the development of collectivity both with particle number and angular momentum. Our IBM calculation with up to four decoupled particles facilitates the understanding of the evolution of structure in the transitional region. The complex decay patterns of the $N > 46$ nuclei change to more regular sequences when $N < 46$ because the lowering of the neutron Fermi surface prevents aligned quasineutron states from being energetically competitive. Deformation and rotation is never the dominant collective mode in $N = 46$ up to spin $J = 24\hbar$, but may be above spin $J = 16\hbar$ in $N = 44$, and certainly is dominant in the ground state of $N = 42$ strontium and zirconium nuclei. The four-quasiparticle configurations which are dominant along the yrast line in $N = 46$ isotones cease to be the yrast states in lighter isotopes. Many interesting problems can be considered in our model framework and are being pursued; for example, we are interested in the mixed neutron-proton configurations which can be explored in odd-A nuclei, and in the manifestation of saturation effects in transition rates. We also feel that our model offers a powerful tool for studying the modification of interactions at higher excitation energies.

D.V. would like to thank the Alexander von Humboldt Foundation for financial support.

[1] E. K. Warburton, J. W. Olness, C. J. Lister, R. W. Zurmuhle, and J. A. Becker, Phys. Rev. C **31**, 1184 (1985).
[2] P. Bonche, H. Flocard, P. H. Heenen, S. J. Krieger, and M. S. Weiss, Nucl. Phys. **A443**, 39 (1985).
[3] M. Girod, J. P. Delaroche, D. Gogny, and J. F. Berger, Phys. Rev. Lett. **62**, 2452 (1989).
[4] D. Bucurescu, G. Cata, D. Cutoiu, G. Constantinescu, M. Ivascu, and N. V. Zamfir, Nucl. Phys. **A401**, 22 (1983).
[5] K. Heyde, J. Moreau, and M. Waroquier, Phys. Rev. C **29**, 1859 (1984).
[6] D. Galeriu, D. Bucurescu, and M. Ivascu, J. Phys. G **12**, 329 (1986).
[7] W. Nazarewica, J. Dudek, R. Bengtsson, T. Bengtsson, and I. Ragnarsson, Nucl. Phys. **A435**, 397 (1985).
[8] J. Dudek, W. Nazarewicz, and N. Rowley, Phys. Rev. C **35**, 1489 (1987).
[9] D. Vretenar, V. Paar, G. Bonsignori, and M. Savoia, Phys. Rev. C **42**, 993 (1990); **44**, 223 (1991).
[10] F. Iachello and D. Vretenar, Phys. Rev. C **43**, R945 (1991).
[11] F. Iachello, Nucl. Phys. **A522**, 83c (1991).
[12] D. Vretenar, G. Bonsignori, and M. Savoia, Phys. Rev. C **47**, 2019 (1993).
[13] P. Chowdhury *et al.*, Phys. Rev. Lett. **67**, 2950 (1991).
[14] D. Ward, Nucl. Phys. **A520**, 139c (1990).
[15] D. J. Blumenthal, C. J. Lister, P. Chowdhury, B. Crowell, P. J. Ennis, Ch. Winter, T. Drake, A. Galindo-Uribarri, D. Zwartz, H. R. Andrews, G. C. Ball, D. Radford, D. Ward, and V. P. Janzen, Phys. Rev. Lett. **66**, 3121 (1991).
[16] H. G. Price, C. J. Lister, B. J. Varley, W. Gelletly, and J. W. Olness, Phys. Rev. Lett. **51**, 1842 (1983).
[17] J. L. Durell, private communication.
[18] C. J. Gross, private communication.
[19] Ch. Winter, D. J. Blumenthal, P. Chowdhury, B. Crowell, P. J. Ennis, S. J. Freeman, C. J. Lister, C. J. Gross, J. Heese, A. Jangclaus, K. P. Lieb, D. Rudolph, M. A. Bentley, W. Gelletly, J. Simpson, J. L. Durell, and B. J. Varley, Nucl. Phys. **A535**, 137 (1991).
[20] A. W. Mountford, J. Billowes, W. Gelletly, H. G. Price, and D. D. Warner, Phys. Lett. B **279**, 228 (1992).
[21] A. M. Mountford, Ph.D. thesis, University of Manchester, 1991.
[22] C. J. Lister *et al.*, in *International Conference on In-Beam Nuclear Spectroscopy,* Debrecen, Hungary, 1984, edited by Z. S. Dombradi and T. Fenyes (Hungarian Academy of Science, Budapest, 1984).
[23] S. Mitarai *et al.*, Z. Phys. A **344**, 405 (1993).
[24] A. Arima and F. Iachello, Ann. Phys. (N.Y.) **99**, 253 (1976); **111**, 201 (1978); **123**, 468 (1979).
[25] F. Iachello and A. Arima, *The Interacting Boson Model* (Cambridge University Press, Cambridge, 1987).
[26] L. S. Kisslinger and R. A. Sorensen, Rev. Mod. Phys. **35**, 853 (1963).
[27] J. Billowes and K. P. Lieb, private communication.
[28] U. Kaup, A. Gelberg, P. Von Brentano, and O. Scholten, Phys. Rev. C **22**, 1738 (1980).
[29] A. M. Mountford and N. Koller (unpublished).
[30] N. V. Zamfir and R. F. Casten, Phys. Lett. B **260**, 265 (1991).